High-Level Expression and Mutagenesis of Recombinant Human Phosphatidylcholine Transfer Protein Using a Synthetic Gene: Evidence for a C-Terminal Membrane Binding Domain†

Li Feng,‡,§ Wayne W. Chan,‡ Steven L. Roderick,|| and David E. Cohen*,‡,||

Departments of Medicine and Biochemistry, Marion Bessin Liver Research Center, Albert Einstein College of Medicine, Bronx, New York 10461

Received May 11, 2000; Revised Manuscript Received September 25, 2000

ABSTRACT: Phosphatidylcholine transfer protein (PC-TP) is a 214-amino acid cytosolic protein that promotes intermembrane transfer of phosphatidylcholines, but no other phospholipid class. To probe mechanisms for membrane interactions and phosphatidylcholine binding, we expressed recombinant human PC-TP in *Escherichia coli* using a synthetic gene. Optimization of codon usage for bacterial protein translation increased expression of PC-TP from trace levels to >10% of the *E. coli* cytosolic protein mass. On the basis of secondary structure predictions of an amphipathic α-helix (residues 198−212) in proximity to a hydrophobic α-helix (residues 184−193), we explored whether the C-terminus might interact with membranes and promote binding of phosphatidylcholines. Consistent with this possibility, truncation of five residues from the C-terminus shortened the predicted amphipathic α-helix and decreased PC-TP activity by 50%, whereas removal of 10 residues eliminated the α-helix, abolished activity, and markedly decreased the level of membrane binding. Circular dichroic spectra of synthetic peptides containing one ($^{196-214}$PC-TP) or both ($^{183-214}$PC-TP) predicted C-terminal α-helices in aqueous buffer were most consistent with random coil structures. However, both peptides adopted α-helical configurations in the presence of trifluoroethanol or phosphatidylcholine/phosphatidylserine small unilamellar vesicles. The helical content of $^{196-214}$PC-TP increased in proportion to vesicle phosphatidylserine content, consistent with stablization of the α-helix at the membrane surface. In contrast, the helical content of $^{183-214}$PC-TP was not influenced by vesicle composition, implying that the more hydrophobic of the α-helices penetrated into the membrane bilayer. These studies suggest that tandem α-helices located near the C-terminus of PC-TP facilitate membrane binding and extraction of phosphatidylcholines.

Phosphatidylcholine transfer protein (PC-TP)[1] is a cytosolic lipid transfer protein that catalyzes in vitro intermembrane exchange as well as net transfer of phosphatidylcholines (PCs) (*1*). Although PC-TP was purified first from bovine liver nearly three decades ago (*1*), the molecular basis for its specificity as well as its physiological function remains unclear. On the basis of its tissue distribution and experiments in models systems, roles for PC-TP have been postulated in hepatocellular transport of biliary PCs (*2*, *3*) as well as in pulmonary surfactant formation (*4*). In a recent study on mice with homozygous disruption of the *Pc-tp* gene, however, van Helvoort et al. (*5*) discounted these possibilities by demonstrating both intact biliary lipid secretion and lung morphology.

Following purification of bovine PC-TP (*6*) and prior to its cDNA cloning (*4*, *7*), considerable efforts were focused on elucidating its biochemical and functional properties (*1*). It was shown that PC-TP specifically recognizes the phos-

† Supported in part by Grant DK48873 (NIH), pilot and feasibility grants from the Liver Research Center at Albert Einstein College of Medicine (DK41296), and the Howard Hughes Medical Institute-Research Resources for Medical Schools (D.E.C.). Support from the Alexandrine and Alexander L. Sinsheimer Fund (D.E.C.) is gratefully acknowledged. L.F. is the recipient of an American Liver Foundation Evelyn and James Silver Memorial, Greater New York Chapter, Postdoctoral Research Fellowship.

* To whom correspondence should be addressed: Liver Research Center, Ullmann 625, Albert Einstein College of Medicine, 1300 Morris Park Ave., Bronx, NY 10461. Phone: (718) 430-2098. Fax: (718) 430-8975. E-mail: dcohen@aecom.yu.edu.

‡ Department of Medicine, Marion Bessin Liver Research Center, Albert Einstein College of Medicine.

§ Present address: Agilix Corp., P.O. Box 8175, New Haven, CT 06530.

|| Department of Biochemistry, Albert Einstein College of Medicine.

[1] Abbreviations: α1, α-helix predicted to span residues 10−20 of human PC-TP; α2, α-helix predicted to span residues 76−92 of human PC-TP; α3, α-helix predicted to span residues 184−193 of human PC-TP; α4, α-helix predicted to span residues 198−212 of human PC-TP; CAI, codon adaptation index; DTT, dithiothreitol; ESI-MS, electrospray injection mass spectrometry; GST, glutathione *S*-transferase; IPTG, isopropyl β-D-thiogalactopyranoside; MOPS, 3-(*N*-morpholino)propanesulfonic acid; ORF, open reading frame; PC, phosphatidylcholine; PC-TP, phosphatidylcholine transfer protein; $^{50-63}$PC-TP, GLYEYKVFGVLEDC; $^{183-214}$PC-TP, IPSWLINWAAKNGVPNFLKDMARACQNYLKKT; $^{196-214}$PC-TP, VPNFLKDMARACQNYLKKT; PE, phosphatidylethanolamine; PMSF, phenylmethanesulfonyl fluoride; PS, phosphatidylserine; SUV, small unilamellar vesicle; TFE, trifluoroethanol; ΔC5, C-terminal truncation of human PC-TP (residues 209−214 deleted); ΔC10, C-terminal truncation of human PC-TP (residues 205−214 deleted); ΔN5, N-terminal truncation of human PC-TP (residues 2−6 deleted); ΔN10, N-terminal truncation of human PC-TP (residues 2−11 deleted).

10.1021/bi001076a CCC: $19.00
Published on Web 11/23/2000

phorylcholine headgroup of PC (*8*). Upon determination of the complete primary structure of bovine PC-TP (*9*), computer-based predictions of secondary structure were combined with photoaffinity labeling and biochemical data (*10*) to postulate the molecular features of a lipid binding site responsible for tight noncovalent binding of PC fatty acyl chains (*11*). On the basis of fluorescence depolarization measurements, it was estimated that PC-TP was generally shaped as a prolate ellipsoid with the sn-1 and sn-2 acyl chains immobilized at approximately 60−90° angles to each other (*12*). Binding assays using fluorescent phospholipid analogs further demonstrated that PC-TP displayed high relative affinities for PCs with sn-1 palmitoyl- and sn-2 unsaturated acyl chains (*1*, *13*). Notwithstanding these and other studies (*1*), mechanisms by which PC-TP mediates PC transfer between membranes remain uncertain.

In recent years, cDNAs containing complete open reading frames (ORFs) have been cloned for bovine (*4*, *7*), mouse (*5*), rat (*14*), and human (*5*, *15*) PC-TPs. The deduced amino acid sequences demonstrate that PC-TPs are highly conserved (>77% identical, >84% similar) (*5*). The availability of these cDNAs provides the opportunity to study structure−function relationships of recombinantly expressed proteins. In a previous study (*16*), we were unable to express recombinant bovine PC-TP using *Escherichia coli*, but demonstrated that a baculovirus/Sf9 cell system could be utilized to produce recombinant rat PC-TP in modest amounts. Here we report expression and characterization of recombinant human PC-TP using both baculovirus and *E. coli*. We demonstrate that high levels of expression may be achieved in *E. coli* using a synthetic gene for PC-TP with codon usage optimized for bacterial protein translation. Analysis of truncation mutants of recombinant human PC-TP suggests that the C-terminus of the protein participates in membrane interactions required for PC transfer activity. This assertion is supported by circular dichroism analysis of synthetic C-terminal peptides and their interactions with model membranes.

MATERIALS AND METHODS

Restriction endonucleases as well as all other routine molecular reagents were purchased from either Boehringer Mannheim (Indianapolis, IN) or Life Technologies (GibcoBRL, Gaithersburg, MD). Oligonucleotides were synthesized by Life Technologies. Grade I egg yolk PC, egg yolk phosphatidylethanolamine (PE), brain phosphatidylserine (PS), and bovine heart cardiolipin were from Avanti Polar Lipids (Alabaster, AL). Phospholipids were >99% pure, as determined by high-performance liquid chromatography (*17*). L-α-1-Palmitoyl-2-linoleoyl[*linoleoyl*-1-^{14}C]PC (58 mCi/mmol), [*cholesteryl*-1,2,6,7-^{3}H(N)]cholesteryl oleate (71 Ci/mmol), and L-α-1-palmitoyl-2-arachidonyl[*arachidonyl*-1-^{14}C]PE (56 mCi/mmol) were from NEN Life Science Products (Boston, MA). Trifluoroethanol (TFE) and other chemicals were ACS or reagent grade and were purchased from Sigma (St. Louis, MO). Human liver cytosol was a generous gift from R. Stockert, Albert Einstein College of Medicine.

Preparation of a cDNA Encoding Human PC-TP

To facilitate expression of recombinant human PC-TP, a cDNA containing a complete ORF was first constructed. A cDNA that partially encodes human PC-TP (Genbank accession number W04200) was identified (*15*) by searching the expressed sequence tag database (dbEST) (*18*) and was purchased from Research Genetics (Hunstville, AL). A cDNA fragment consisting of the remaining 5′ nucleotide sequence of the ORF was previously cloned in our laboratory by 5′ rapid amplification of cDNA ends (GenBank accession number AF114430) (*15*). These two cDNA molecules were joined at a common *Sma*I restriction endonuclease site within the general purpose cloning vector pBluescript KS (Stratagene Cloning Systems, La Jolla, CA) to create a full-length (642 bp) ORF. Appropriate construction of the cDNA clone encoding human PC-TP was verified by nucleotide sequencing.

Expression of Recombinant Human PC-TP Using Baculovirus

Baculovirus Preparation and Recombinant Protein Expression. Recombinant human PC-TP baculovirus was prepared as previously described (*16*) employing the Bac-to-Bac baculovirus expression system (GibcoBRL). As a control, we utilized a baculovirus recombinant for a cDNA encoding a 65 kDa fusion protein of murine IgG2a and *Helicobacter pylori* urease B (generous gift from A. Christ and R. Blumberg, Brigham and Women's Hospital, Boston, MA). Recombinant proteins were expressed by infecting *Spodoptera frugiperda* (Sf9) cells and then harvested in cytosolic preparations as previously described (*16*).

Purification of Recombinant Human PC-TP. Our purification strategy was based on an earlier method developed by Westerman, Kamp, and Wirtz for purifying PC-TP from bovine liver (*19*). Cytosolic proteins (25 mL) prepared from 500 mL infected Sf9 cell cultures were dialyzed against 4 mM sodium phosphate (pH 7.2), 5 mM β-mercaptoethanol, and 3 mM NaN_3 and applied to a 5 mL prepacked HiTrapQ anion exchange column (Amersham Pharmacia Biotech, Piscataway, NJ) equilibrated with the same buffer. Unbound proteins were removed by washing with 4 bed volumes of buffer, and then bound proteins were eluted using a 0 to 200 mM NaCl gradient in buffer (20 bed volumes) at a flow rate of 5 mL/min. Fractions containing PC transfer activity (please see below) were pooled and dialyzed against buffer consisting of 6 mM citric acid and 10 mM potassium phosphate buffer (pH 4.8) and applied to a 5 mL prepacked HiTrapSP cation exchange column (Amersham Pharmacia Biotech) equilibrated with this buffer. Bound proteins were eluted using a linear gradient (20 gel bed volumes) from 6 mM citric acid and 10 mM potassium phosphate (pH 4.8) to 60 mM citric acid, 100 mM potassium phosphate, and 500 mM NaCl (pH 4.8) at a flow rate of 5 mL/min. Reverse-phase HPLC was used as previously described (*16*) to remove salts and minor protein impurities in preparation for mass spectrometry (see below).

Expression of Recombinant Human PC-TP in E. coli

Bacterial expression plasmids were prepared which contained either the native PC-TP cDNA described above or a codon-optimized synthetic cDNA.

Native PC-TP cDNA. To clone the native cDNA into a pET11a bacterial T7 expression vector (Novagen, Madison,

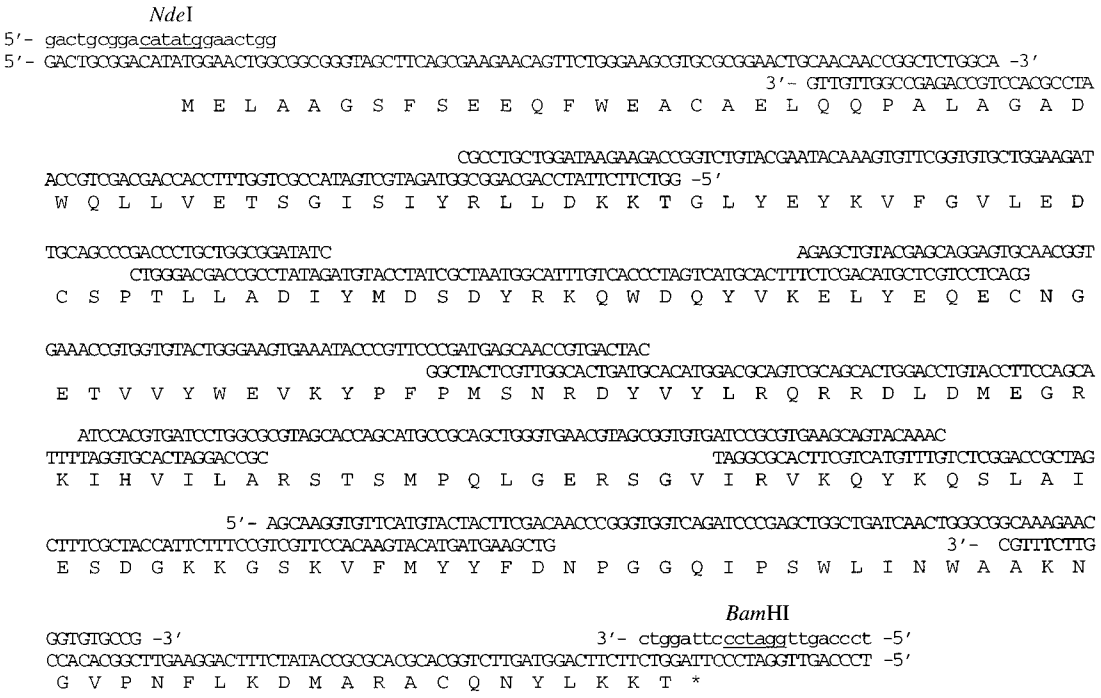

FIGURE 1: Sequences of 10 overlapping oligonucleotides used to construct a 672 bp cDNA comprised of the human PC-TP ORF and cloning sites. Shorter oligonucleotides used as primers for PCR amplification of the synthetic gene are indicated with lowercase letters. The amino acid sequence of human PC-TP is shown below the coding region. The asterisk indicates a stop codon. Restriction endonuclease recognition sequences used for cloning the synthetic gene into the pET11a bacterial expression vector are underlined.

WI), sense (5′-GACTGCGGACATATGGAGCTGGCCGCC-3′) and antisense (5′-TCCCAGTTGGATCCCTTAGGTTT-TCTTGAGGTAG-3′) oligonucleotide primers containing *Nde*I and *Bam*HI restriction sites, respectively, were utilized for amplification of the ORF of PC-TP. PCR conditions were 3 min at 94 °C to denature, followed by four cycles of 55 °C for 1 min, 72 °C for 2 min, and 94 °C for 1 min, followed by 20 cycles of 65 °C for 1 min, 72 °C for 2 min, and 94 °C for 1 min, followed by a final annealing step at 65 °C for 1 min, and a final elongation step at 72 °C for 10 min. The PCR product was digested with *Nde*I and *Bam*HI, gel purified, and subcloned into pET11a, which had been linearized using the same restriction endonucleases. Following verification of the nucleotide sequence, the recombinant plasmid was transformed into *E. coli* strain BL21(DE3) (Novagen).

Synthetic Codon-Optimized PC-TP cDNA. A cDNA encoding human PC-TP but with codon usage optimized for protein expression in *E. coli* (*20*) was synthesized using a recursive PCR strategy described by Dillon and Rosen (*21*). Ten oligonucleotides (five sense and five antisense) ranging in length from 82 to 90 bp were synthesized (Figure 1). Overlapping nucleotide sequences 18−27 bp in length were designed so that their melting temperatures were similar (62−64 °C). To create the synthetic cDNA, 4 pmol of each oligonucleotide was mixed in 50 μL of 2.5 mM $MgCl_2$ and 0.25 mM dNTPs together with 1 unit of *Taq* DNA polymerase (Boehringer Mannheim). Conditions for PCR were 1 min at 80 °C to denature, followed by 12 cycles of 95 °C for 1 min, 55 °C for 1 min, and 72 °C for 2 min, followed by a final denaturing step at 95 °C for 1 min, a final annealing step at 55 °C for 1 min, and a final elongation step at 72 °C for 5 min. The synthetic cDNA was amplified using 22 bp sense and antisense oligonucleotide primers (Figure 1) which contained *Nde*I and *Bam*HI restriction endonuclease sites, respectively. Ten μL of the initial PCR mixture was mixed with 100 pmol of each oligonucleotide primer in 50μL of 2 mM $MgCl_2$ and 0.25 mM dNTPs plus 1 unit of high fidelity *Pwo* DNA polymerase (Boehringer Mannheim). PCR conditions were 1 min at 80 °C to denature, followed by 30 cycles of 95 °C for 1min, 65 °C for 1min, and 72 °C for 2min, followed by a final denaturing step of 95 °C for 1 min, a final annealing step of 65 °C for 1 min and a final elongation step at 72 °C for 5 min. The PCR product was gel purified, ligated into pGEM-Easy TA cloning vector (Promega, Madison, WI), and transformed into *E. coli* SoloPack Gold supercompetent cells (Stratagene). The codon-optimized synthetic human PC-TP cDNA was excised from pGEM-Easy with *Nde*I and *Bam*HI and subcloned into PET11a digested with the same endonucleases. Following amplification in *E. coli* strain DH5α and nucleotide sequencing, which confirmed the desired sequence, the recombinant plasmid was transformed into *E. coli* strain BL21(DE3).

Expression of Recombinant PC-TP. Bacterial cultures were grown from single colonies in 250 mL of LB containing 75 μg/mL carbenicillin at 37 °C until OD_{600} values ranging from 0.4 to 0.6 were reached. Expression of recombinant PC-TP was induced by addition of isopropyl β-D-thiogalactopyranoside (IPTG) to a final concentration of 1 mM, followed by overnight incubation at room temperature with gentle shaking (120 rpm). Bacteria were harvested by centrifugation (5000*g* for 15 min at 4 °C) and resuspended in 20 mL of buffer consisting of 12 mM sodium phosphate (pH 6.2), 1 mM EDTA, 5 mM EGTA, 5 mM dithiothreitol (DTT), 3 mM NaN_3, and 1 mM PMSF. Soluble cytosolic proteins were harvested by sonication and ultracentrifugation (*16*).

Protein Purification. Cytosolic preparations from *E. coli* were diluted 3-fold into 4 mM sodium phosphate buffer (pH 6.2) containing 5 mM DTT and 3 mM NaN_3 and applied to a 5 mL prepacked HiTrapQ anion exchange column equili-

brated with the same buffer. Bound proteins were eluted with 20 bed volumes of a linear 0 to 200 mM NaCl gradient at a flow rate of 5 mL/min. In preparation for mass spectrometry (see below), recombinant PC-TP was further purified by reverse-phase HPLC (*16*).

Expression and Purification of Truncated Recombinant Human PC-TPs. To create truncation mutations, the synthetic PC-TP cDNA (Figure 1) was used as a template for PCR preparation of cDNAs with suitable restriction sites for cloning into pET11a and pET19b (Novagen) as well as pGEX-KG (Amersham Pharmacia Biotech). Five or 10 amino acids were deleted from either the N-terminus, ΔN5 (residues 2−6 deleted) or ΔN10 (residues 2−11 deleted), or the C-terminus, ΔC5 (residues 210−214 deleted) or ΔC10 (residues 205−214 deleted). For PCR amplification of wild-type and C-terminally truncated PC-TP cDNAs, a sense oligonucleotide primer (5′-TTGGATCCCATATGGAACTG-GCGGCGGGTAG-3′) containing *Bam*HI and *Nde*I restriction sites was paired with either 5′-TCCCAGTTGGATC-CCTTAGG-3′ (wild type), 5′-CAGGATCCCTTAGTTCT-GGCACGCACGCGCCAT-3′ (ΔC5), or 5′-AAGGATC-CCTTACGCCATATCTTTCAGGAAGTTC-3′ (ΔC10) antisense oligonucleotide, each of which also contained a *Bam*HI restriction site. For preparation of N-terminally truncated mutants, sense oligonucleotide primers 5′-TTG-GATCCCATATGAGCTTCAGCGAAGAACAGTTC-3′(ΔN5) and 5′-TTGGATCCCATATGCAGTTCTGGGAAGCGTG-CGC-3′ (N10) containing *Bam*HI and *Nde*I restriction sites were each paired with an antisense primer 5′-TCCCAGT-TGGATCCCTTAGG-3′ containing a *Bam*HI restriction site. PCR conditions were six cycles of 94 °C for 3 min, 55 °C for 1 min, and 72 °C for 2 min and then 25 cycles of 94 °C for 3 min, 65 °C for 1 min, and 72 °C for 2 min. DNA fragments encoding mutated as well as wild-type PC-TPs were digested with *Nde*I with *Bam*HI or *Bam*HI alone, gel purified, and then ligated into pET11a and pET19b digested with *Nde*I with *Bam*HI or pGEX-KG digested with *Bam*HI alone, respectively. Recombinant plasmids were transformed into *E. coli* strain DH5α. Following confirmation of their nucleotide sequences, plasmids were then transformed into *E. coli* strain BL21(DE3).

Expression and Purification of Mutated PC-TPs. Cultures of *E. coli* strain BL21(DE3) were grown in LB containing carbenicillin (75 μg/mL) until the OD_{600} reached 0.4−0.6, at which point protein expression was induced by addition of IPTG (1 mM final concentration). Bacteria were incubated overnight at room temperature and then harvested by centrifugation.

GST fusion proteins produced with pGEX-KG were purified using a GST purification module (Amersham Pharmacia Biotech) according to the manufacturer's specifications. Cytosolic proteins were prepared from 1 L cultures by sonication and ultracentrifugation (*16*). Briefly, 0.3 mL of glutathione Sepharose 4B was added to the cytosolic preparations (∼20 mL), gently shaken at 22 °C for 30 min, and then pelleted by centrifugation at 600*g*. After being washed with 20 mM phosphate buffer (pH 7.2), gel slurries were transferred to columns and buffer solutions were drained. Any additional unbound proteins were removed with two washes (3 column volumes each) of the same buffer. GST fusion proteins were eluted by three applications to each column of 0.3 mL of 10 mM reduced glutathione in 50 mM Tris-HCl (pH 8.0). Cleavage of GST from recombinant PC-TPs was accomplished by thrombin digestion (1 unit) at room temperature for 16 h. GST was removed from the reaction mixture by overnight incubation with 0.1 mL of glutathione Sepharose 4B at 4 °C, followed by centrifugation.

Because preliminary experiments demonstrated that GST fusion proteins were not overexpressed using the synthetic gene, we utilized pET19b to produce wild-type and mutated PC-TPs in the form of His-tag fusion proteins for membrane binding studies (see below), which required larger quantities of purified protein. His-tag proteins were purified from soluble bacterial proteins prepared by addition of 5 mL of BugBuster protein extraction reagent (Novagen)/g of bacteria and then ultracentrifugation at 100000*g* for 0.5 h at 4 °C. This was followed by addition of 3 mL of TALON metal affinity resin (Clontech)/g of bacteria equilibrated with buffer [20 mM Tris-HCl, 300 mM NaCl, 1 mM NaN_3, 10 mM 2-mercaptoethanol, 0.5 mM PMSF, and 10% glycerol (pH 7.5)] containing 5 mM imidazole. Following incubation for 1 h at 4 °C, the resin was pelleted at 900*g* for 5 min and then washed three times (3 resin volumes/wash) with buffer containing 30 mM imidazole. His-tag fusion proteins were eluted by incubation for 1 h at 4 °C with 3 resin volumes of buffer containing 300 mM imidazole. Proteins were dialyzed against 10 mM Tris-HCl, 20 mM NaCl, 1 mM DTT, and 1 mM NaN_3 and were stored at 4 °C for up to 2 days. Prior to experiments, His-tag fusion proteins were dialyzed against 10 mM 3-(*N*-morpholino)propanesulfonic acid (MOPS) and 1 mM DTT (pH 7.4).

Peptide Synthesis

The C-terminal peptides VPNFLKDMARACQNYLKKT ($^{196-214}$PC-TP) and IPSWLINWAAKNGVPNFLKDMAR-ACQNYLKKT ($^{183-214}$PC-TP) and the internal peptide GLYEYKVFGVLEDC ($^{50-63}$PC-TP) were synthesized by solid-phase fluorenylmethoxycarbonyl chemistry using an Applied Biosystems 433A peptide synthesizer (Laboratory for Macromolecular Analysis, Albert Einstein College of Medicine). Peptides were purified by reverse-phase HPLC (Vydac 218TP C18 column MetaChem Technologies, Torrance, CA), and molecular weights were confirmed by mass spectroscopy (see below).

Antibody Production

Recombinant human PC-TP expressed using baculovirus was purified as described above and used as an antigen to produce rabbit anti-human PC-TP polyclonal antiserum (Covance Research Products, Denver, PA). For detection of truncated PC-TPs, polyclonal antibodies were raised to $^{50-63}$PC-TP. Using the C-terminal cysteine residue as a linker, the peptide was covalently attached (Princeton Biomolecules, Columbus, OH) to maleimide-activated keyhole limpet hemocyanin (Pierce, Rockford, IL). The keyhole limpet hemocyanin-linked peptide was used as an antigen to produce rabbit anti-$^{50-63}$PC-TP polyclonal antiserum (Covance Research Products).

Small Unilamellar Vesicles (SUVs)

Phospholipids dissolved in chloroform were combined in PC:PS molar ratios of 100:0, 90:10, 80:20, and 70:30. Lipid mixtures were dried under a stream of nitrogen and then

resuspended in 10 mM MOPS at pH 7.4. SUVs (5 mM phospholipid) were prepared by bath sonication (Special Ultrasonic Cleaner, Laboratory Supply Corp., Hicksville, NY) as previously described (*16*).

Assay of Phospholipid Transfer Activity

Phospholipid transfer activity of recombinant expressed proteins (nanomoles per hour) was determined in vitro by measuring the rates of protein-mediated transfer of [^{14}C]PC or [^{14}C]PE from SUV to multilamellar vesicles as previously described (*16*). In this assay, [^{3}H]cholesteryl oleate incorporated into SUV was nonexchangeable and served as a standard for calculation of transfer activities.

Peptide−Membrane Interactions

Interactions between synthetic peptides and model membranes were characterized by circular dichroism. Circular dichroic spectra were obtained at 25 °C using a JASCO J-710 spectropolarimeter (JASCO Inc., Easton, MD) fitted with a 2 mm circular quartz cell. Circular dichroism was measured at wavelengths ranging from 190 to 260 nm in 0.5 nm increments at a rate of 50 nm/min, with a response of 1 s and a bandwidth of 1.0 nm. Samples were prepared essentially as described by Huang et al. (*22*). Briefly, 50 μL of solutions containing peptides dissolved in water (150 μM) was mixed with 50 μL of SUVs or 10 mM MOPS (pH 7.4) and 400 μL of water or a TFE/water mixture (62.5:37.5, v:v). In all experiments, the final concentrations of peptide and phospholipid were 15 μM and 0.5 mM, respectively. Mixtures (500 μL) were incubated at room temperature for 10 min prior to measurements. Background was determined using buffer or SUV alone. For each measurement, four to six scans were averaged and smoothed. Helical contents of peptides were calculated (*22*) from the mean residue molar ellipticity [θ] (degrees per square centimeter per decimole) at 222 nm (θ_{222}) according to the equation $\theta_{222} = (f_h - i\kappa/N)[\theta_{h222\infty}]$. In this equation, f_h represents the fraction of the N residues of the peptide which are in a helical configuration. The number of helices in the peptide is denoted by *i*. The constants κ and $\theta_{h222\infty}$ have values at 222 nm of 2.6 and −39500 deg cm^2 dmol^{-1}, respectively. In preliminary experiments, micellization of SUVs by amphipathic peptides was excluded by quasielastic light scattering spectroscopy (*23*), which demonstrated no changes in SUV sizes following incubation with peptides.

Protein−Membrane Interactions

Binding of wild-type and mutated recombinant human PC-TPs was assessed by minor modification of an assay described by Huang et al. (*22*). Solutions containing purified recombinant proteins in 10 mM MOPS (pH 7.4) were mixed together with SUV (PC:PS molar ratio of 80:20) to a final volume of 200 μL. The final protein concentration (5 μM) was held constant, whereas the SUV phospholipid concentration was varied (0−860 μM) to achieve phospholipid:protein molar ratios of 0−170. Mixtures were incubated for 10 min at room temperature to allow binding of proteins to SUVs, and then unbound proteins were collected by ultrafiltration through a Microcon YM100 100 kDa molecular mass cutoff filter (Millipore, Bedford, MA) by centrifugation at 3000*g* for 5 min. Unbound proteins remaining within the filter were eluted by centrifugation (3000*g* for 2 min) of an addition 100 μL of 10 mM MOPS, and were combined with initial ultrafiltrates. Aliquots (10−20 μL) of ultrafiltrates containing unbound proteins were transferred to PVDF membranes (Immobilon-P, Millipore) using a slot−blot apparatus (The Convertible Filtration Manifold System, GibcoBRL) and probed with a 1:5000 dilution of anti-$^{50-63}$PC-TP antibody. Detection was achieved via enhanced chemiluminescence (New England Nuclear, Boston, MA) with a 1:25000 dilution of goat anti-rabbit horseradish peroxidase-conjugated secondary antibody (Bio-Rad Laboratories, Hercules, CA). Scanning laser densitometry and image analysis using ImageQuant software (Molecular Dynamics, Sunnyvale, CA) were utilized to quantify the intensities of protein bands.

Analytical Techniques

Protein concentrations were determined by the method of Bradford (*24*) using a reagent from Bio-Rad and bovine serum albumin as a standard. For purified recombinant PC-TPs, concentrations were also determined from OD_{280} values using molar extinction coefficients calculated on the basis of primary structures. Protein purities were assessed by sodium dodecyl sulfate−polyacrylamide gel electrophoresis (SDS−PAGE) (*25*), with relative intensities of protein bands visualized by Coomassie brilliant blue staining and quantified by scanning laser densitometry and image analysis using ImageQuant software. The isoelectric point was determined by two-dimensional electrophoresis (Multiphor II flatbed electrophoresis system, Amersham Pharmacia Biotech). Molecular masses of purified recombinant proteins and synthetic peptides were determined by electrospray injection mass spectrometry (ESI-MS) using a Voyager RP Biospectrometry Work Station (Perseptive Biosystems, Framingham, MA). Plasmid DNA was sequenced by fluorescence cycle sequencing (Applied Biosystems model 377 automated sequencer, Perkin-Elmer, Foster City, CA). A Precise 494 protein sequencer (Perkin-Elmer Applied Biosystems) was utilized for amino acid sequencing. Nucleotide and amino acid sequences were analyzed using DNAsis software (Hitachi Genetic Systems, South San Francisco, CA). The secondary structure for human PC-TP was predicted using the Pred2ary algorithm (http://www.cmpharm.ucsf.edu/~jmc/pred2ary/) developed by Chandonia and Karplus (*26*).

RESULTS

Expression and Characterization of Recombinant PC-TP Expressed Using Baculovirus. PC transfer activity was present in cytosolic preparations from Sf9 cells following infection with recombinant human PC-TP, but not recombinant control, baculovirus. Substitution of [^{14}C]PE for [^{14}C]-PC resulted in the loss of transfer activity for Sf9 cells infected with recombinant PC-TP baculovirus. The identity of recombinant human PC-TP was confirmed by amino acid sequencing, by ESI-MS, and by two-dimensional electrophoresis, which demonstrated that the isoelectric point (pI) of purified recombinant PC-TP (5.3) corresponded well to the predicted value of 5.5. Recombinant PC-TP accounted for ~8% of the cytosolic protein mass of infected Sf9 cells. Overall, the yield of purified recombinant PC-TP from 10

mg of cytosolic protein was ~500 μg. By Western blot analysis (data not shown), anti-recombinant human PC-TP antibodies reacted with purified recombinant PC-TP, recombinant PC-TP in crude cytosol of recombinant PC-TP-infected Sf9 cells, and a 25 kDa band in human liver cytosol, but not recombinant control-infected cytosol.

Expression of Recombinant Human PC-TP Using E. coli. The potential for a bacterial expression system to increase yield and facilitate mutagenesis prompted us to re-evaluate *E. coli* for production of recombinant human PC-TP (*16*). In preliminary experiments, protein expression using the native PC-TP ORF cloned into pET11a resulted in a faint 25 kDa protein band by SDS−PAGE, which was immunoreactive as determined by Western blot analysis (not shown). Low levels of PC but not PE transfer activity were detected in cytosolic preparations. Although these findings suggested that recombinant human PC-TP was expressed in *E. coli*, systematic variations in duration and temperature used for IPTG induction failed to improve expression levels.

Figure 1 displays the five sense and five antisense oligonucleotides utilized for PCR synthesis of a cDNA with codon usage optimized for expression in *E. coli*, as well as the deduced amino acid sequence of human PC-TP. Following PCR synthesis and amplification, the cDNA was cloned into pGEM-Easy for nucleotide sequence verification. cDNAs purified from each of 20 separate clones contained mismatches between the intended and observed nucleotide sequences. Typically, short (~5−10 bp) segments of DNA were deleted, possibly due to secondary structures that may have formed in the long oligonucleotides during the primary PCR. One clone contained only two minor discrepancies compared with the intended sequence. One of these was substitution of C for T at nucleotide 183. This did not alter the deduced amino acid (i.e., F60) and did not appreciably reduce the codon usage frequency (*27*). The other discrepancy was deletion of C at nucleotide 225. This was corrected by using site-directed mutagenesis (QuickChange mutagenesis kit, Stratagene).

Figure 2A shows SDS−PAGE analysis of *E. coli* cytosolic proteins before and following induction of recombinant PC-TP expression using either the native or synthetic cDNA. The synthetic cDNA resulted in overexpression (>10% of soluble protein) of an appropriately sized (~25 kDa) band. Western blot analysis (not shown) confirmed that the overexpressed band was immunoreactive with anti-recombinant human PC-TP antiserum and that PC-TP was expressed at lower levels using the native cDNA. In preliminary experiments using the synthetic cDNA, expression of soluble recombinant PC-TP was optimized when IPTG-induced bacterial cultures were grown overnight at room temperature. In contrast, growth of *E. coli* at 37 °C was associated with marked increases in insoluble PC-TP, which was present in the bacterial pellet following sonication and ultracentrifugation (data not shown). Although this insoluble fraction could be purified from inclusion bodies and resolubilized in 6 M guanidine-HCl, standard protocols for protein refolding (*28*) did not yield active PC-TP. Figure 2B shows PC transfer activity in the soluble protein fraction following induction of the native and synthetic cDNAs, as well as in control *E. coli* cytosol for which PC transfer activity was not detected. Consistent with marked overexpression of PC-TP using the synthetic gene, PC transfer activity increased much more sharply to approach its maximal value than PC-TP expressed using the native cDNA.

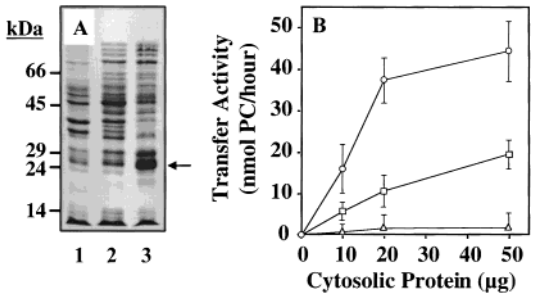

FIGURE 2: Expression of recombinant human PC-TP using *E. coli*. (A) Overexpression of PC-TP using a synthetic cDNA with codon usage optimized for *E. coli*. SDS−PAGE analysis and Coomassie brilliant blue staining of soluble bacterial proteins prior to and following overnight induction (1 mM IPTG) at room temperature. Each lane was loaded with 25 μg of protein. Prior to induction, bacteria transformed with either the native or the synthetic cDNA cloned into a pET11a bacterial expression vector yielded the result shown in the preinduction lane (lane 1). Following induction, the synthetic (lane 3) but not the native (lane 2) PC-TP plasmid resulted in overexpression of recombinant human PC-TP (indicated by the arrow). (B) Intermembrane PC transfer activity was determined for *E. coli* cytosolic proteins harvested prior to induction (△), following induction of strains harboring overexpression plasmids containing either the native (□) or synthetic (○) nucleotide sequences corresponding to PC-TP.

Recombinant PC-TP was purified (>95%) from the soluble protein fraction of a sonicated bacterial lysate by anion exchange chromatography. ESI-MS revealed a molecular mass of 24 842 ± 1 Da, which precisely matched the predicted molecular mass of 24 842 Da. Amino acid sequencing of the N-terminus revealed an exact match to the first 13 amino acids of human PC-TP. The yield of recombinant human PC-TP expressed in *E. coli* using the synthetic gene was ~5 mg of purified protein per liter of bacterial culture.

Mutational Analysis of Recombinant PC-TP. The synthetic cDNA was used to prepare truncation mutations. Expression of mutated PC-TPs as GST fusion proteins facilitated their purification, and this permitted direct comparisons of PC transfer activity. Figure 3 demonstrates the influence of mutations on PC-TP activity prior to and following removal of GST. Activities of wild-type and mutated PC-TPs were similar in the presence or absence of GST covalently bound to N-termini. In addition, activity of the wild-type PC-TP expressed by this method was very similar to that of PC-TP purified without the assistance of the GST tag. Deletion of five residues from the N- and C-termini decreased activity by 10 and 50%, respectively, compared to that of wild-type PC-TP (GST removed). Deletion of 10 residues from either the N- or C-terminus of PC-TP eliminated PC transfer activity.

To further probe the possible influence on activity of expressing PC-TPs as fusion proteins, the same mutations were also expressed using pET11a or pET19b expression vectors. Retention of the initial methionine (M) residue for N-terminal truncations permitted expression of proteins without an affinity tag using pET11a. Following induction of protein expression, Western blot analysis demonstrated similar expression levels of recombinant proteins in cytosolic fractions from *E. coli*, and measurements of PC transfer activity using equal amounts cytosolic protein (200 μg) varied

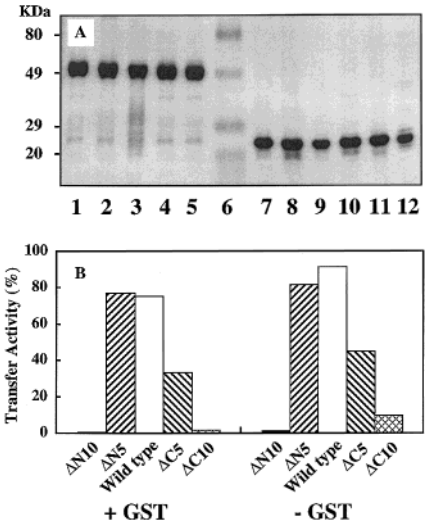

FIGURE 3: Expression in *E. coli* cells of recombinant wild-type and mutated PC-TPs as GST fusion proteins. Starting with the synthetic cDNA (Figure 1), wild type or PC-TPs with truncation mutation were prepared, expressed, and purified as a GST fusion protein. N-Terminal and C-terminal truncations lacked 10 (ΔN10 and ΔC10) or 5 (ΔN5 and ΔC5) amino acids as described in the text. (A) Purified proteins (3 μg) were subjected to SDS−PAGE followed by Coomassie brilliant blue staining. Lanes 1−5 show GST fusion proteins of ΔN10, ΔN5, wild type, ΔC5, and ΔC10. Molecular mass markers are in lane 6. Fusion proteins were cleaved using thrombin, and PC-TPs were purified from GST. Lanes 7−11 contain purified PC-TPs corresponding to lanes 1−5, respectively. Lane 12 is PC-TP expressed and purified without the use of GST (see the text for details). (B) Intermembrane PC transfer activity was determined for equal amounts (3 μg) of mutated and wild-type PC-TP prior to (+GST) and following (−GST) removal. Transfer activity is expressed as a percent of PC transfer activity for the same amount of PC-TP purified without the use of GST. Values represent means for two determinations.

in a manner similar to that of the measurements observed in Figure 3 (data not shown). Despite the 23-amino acid His-tag that was fused to N-termini of recombinant PC-TPs, the same influence of N- and C-terminal truncations was also observed for His-tag fusion proteins purified (>98%) following expression using pET19b.

To explore the possibility that loss of PC transfer activity could be due to aggregation of mutated proteins in solution, purified His-tag fusion proteins (molecular mass of 26404−27610 Da) were subjected to ultrafiltration through Microcon YM50 50 kDa molecular mass cutoff filters (Millipore). No reductions in concentrations (5 μM in 10 mM MOPS at pH 7.4) of wild-type or mutated PC-TPs were detected following ultrafiltration, indicating that truncation mutations did not result in aggregation of PC-TPs over the range of concentrations utilized in this study.

Design of PC-TP C-Terminal Peptides. Computer-based analysis of the deduced 214-amino acid sequence of human PC-TP (Figure 1) predicted four α-helices: α1 (residues 10−20), α2 (residues 76−92), α3 (residues 184−193), and α4 (residues 198−212). Amphiphilicity of each putative α-helix was characterized according to the method of Eisenberg (*29*). Briefly, normalized consensus values for amino acid hydrophobicity (*29*) were used to calculate both the mean hydrophobicity and the helical hydrophobic moment. Figure 4 shows an Eisenberg plot, which uses these values to predict whether an α-helix is likely to reside at a polar−nonpolar interface (region I), within a globular protein (region II) or

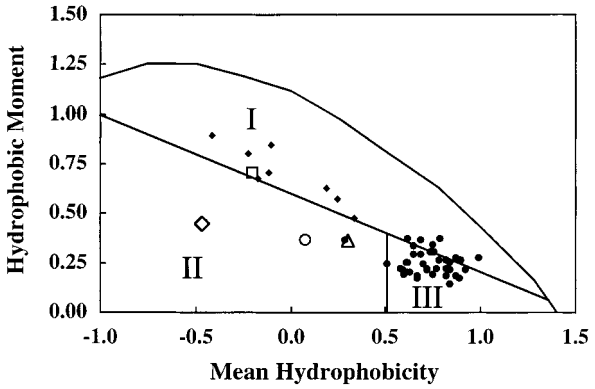

FIGURE 4: Eisenberg plot (*29*) of the hydrophobic moment vs mean hydrophobicity for α-helices. Calculated values are plotted within one of three regions. Region I is characteristic for α-helices which align at a polar−nonpolar interface. Region II is characteristic for α-helices contained within globular proteins. Region III is characteristic for membrane-spanning α-helices. Values for the four predicted α-helices of PC-TP (see the text) are plotted as follows: α1 (residues 10−20) (○), α2 (residues 76−92) (◇) α3 (residues 184−193) (△), and α4 (residues 198−212) (□). The format and values for experimentally confirmed transmembrane (●) and surface-seeking (◆) helices were replotted with permission from Eisenberg et al. (*30*).

as a membrane-spanning domain (region III). The predicted α-helices α1 and α2 of PC-TP fell well within region II. Although α3 also plotted in region II, its coordinates were close to region III, as evidenced by the scatter of data points for verified membrane-spanning helices that were originally used to define the boundary between regions II and III (*30*). The α-helix in proximity to the C-terminus (α4) plotted in region I, suggesting that it should align at a membrane surface.

To explore a potential role for the C-terminus of PC-TP in membrane binding, we synthesized peptides $^{196-214}$PC-TP and $^{183-214}$PC-TP. The shorter (19 amino acids) peptide $^{196-214}$PC-TP, which includes the α-helix closest to the C-terminus (α4), had a net charge of +1. The longer (32 amino acids) $^{183-214}$PC-TP included both α-helices in proximity to the C-terminus, and had a net charge of +2. The predicted helical contents (*26*) of $^{196-214}$PC-TP and $^{183-214}$PC-TP were 79% (15 helical residues and 4 nonhelical residues) and 78% (25 helical residues and 7 nonhelical residues), respectively.

Secondary Structure of PC-TP C-Terminal Peptides. The secondary structure for PC-TP C-terminal peptides was determined by circular dichroism (Figure 5A) in aqueous buffer and in a TFE/buffer mixture (1:1, v:v), which favors intramolecular hydrogen bonding and helix formation (*22*, *31*). The circular dichroic spectrum for $^{196-214}$PC-TP in buffer exhibited a large minimum at 200 nm, consistent with a random coil conformation of low helical content (22.3 ± 2.3%, mean ± SD). However, the presence of TFE dramatically changed the circular dichroic spectrum for this peptide to one characteristic of an α-helix, with minima of 208 and 220 nm. Under these conditions, the helical content of $^{196-214}$PC-TP was 73.6 ± 0.3%, which is close to the predicted value of 79%. The peptide $^{183-214}$PC-TP in aqueous buffer yielded a circular dichroic spectrum intermediate between a random coil conformation and an α-helix, with a minimum at 205 nm and a helical content of 36.0 ± 1.3%. As observed for $^{196-214}$PC-TP, addition of TFE promoted α-helix formation for $^{183-214}$PC-TP with a helical content

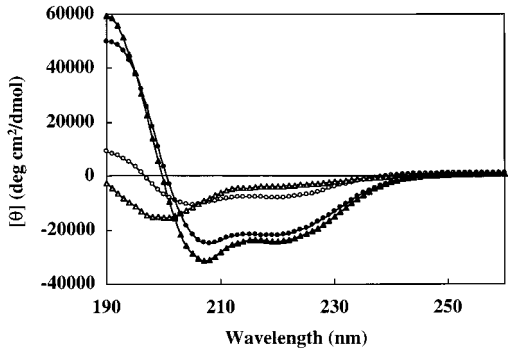

FIGURE 5: Circular dichroism of PC-TP C-terminal peptides (15 μM) in aqueous solution and in TFE. Molar ellipticity was determined for $^{196-214}$PC-TP (triangles) and $^{183-214}$PC-TP (circles) in buffer (white symbols) or in a 1:1 TFE/buffer mixture (black symbols).

(70.1 ± 0.4%) approaching to the predicted value (78%).

Interactions between PC-TP C-Terminal Peptides and Small Unilamellar Vesicles (SUVs). Circular dichroism was also used to characterize the interactions between SUVs and $^{196-214}$PC-TP or $^{183-214}$PC-TP. Panels A and B of Figure 6 show that for both peptides, the presence of SUV altered the secondary structure significantly, yielding circular dichroic spectra indicative of α-helix formation. The influence of SUV composition on peptide helical content is quantified in Figure 6C. For $^{196-214}$PC-TP, the helical content increased linearly as a function of SUV PS content (0−20 mol %) and then leveled off at a helical content near 80%. For $^{183-214}$PC-TP, there was an abrupt increase in helical content upon addition of SUV composed of pure PC to 66.4 ± 3.5%. Addition of PS did not further increase the helical content of $^{183-214}$PC-TP. For both peptides, the maximum helical contents observed in the presence of SUVs were consistent with both computer-predicted values (see above) and circular dichroism measurements in the presence of TFE (Figure 5).

Interactions between Recombinant Proteins and Small Unilamellar Vesicles (SUVs). Figure 7 shows the influence of C-terminal truncations on the predicted secondary structure of PC-TP. Removal of five amino acids, which reduced PC transfer activity by 50% (Figure 3B), shortened the predicted length of the C-terminal helix (α4), whereas removal of 10 amino acids, which eliminated PC transfer activity (Figure 3B), essentially eliminated α4. To determine whether deletion of α4 impaired interactions between PC-TP and membranes, we assessed binding of wild-type and mutated proteins to SUVs. Figure 8 demonstrates the influence of 10-amino acids truncations on binding of PC-TP to SUVs with a membrane composition (80:20 PC:PS molar ratio) that promoted maximal helix formation for α4 (Figure 6A,C). The level of binding of ΔC10 to SUVs was markedly reduced compared with that of wild-type PC-TP, whereas binding of ΔN10 was preserved.

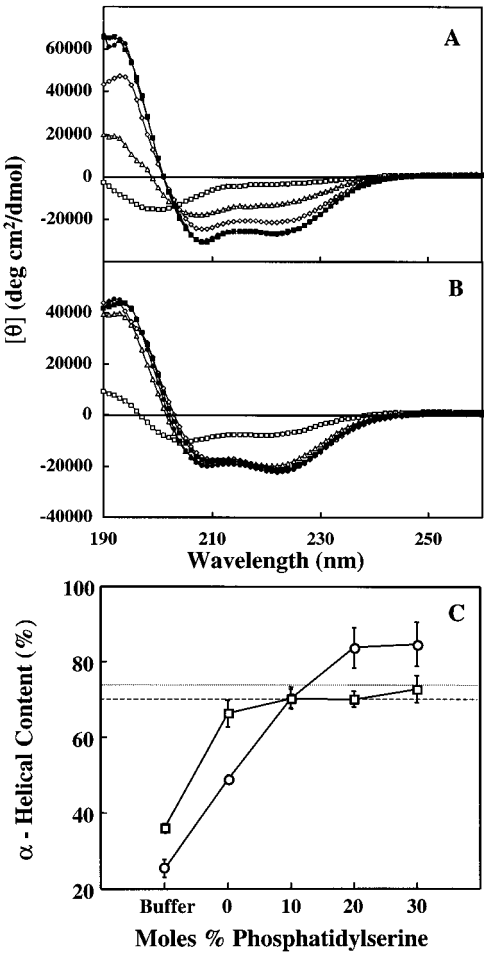

FIGURE 6: Influence of SUV on circular dichroism of PC-TP C-terminal peptides. Molar ellipticity was measured for (A) $^{196-214}$PC-TP (15 μM) and (B) $^{183-214}$PC-TP (15 μM) in the presence of buffer (□) or SUVs (0.5 mM phospholipid) with increasing PS contents: 100:0 (△), 90:10 (◇), 80:20 (■), and 70:30 PC:PS molar ratios (●). (C) Influence of SUV PS content on helical content of $^{196-214}$PC-TP (○) and $^{183-214}$PC-TP (□) calculated from circular dichroism measurements in panels A and B, respectively, as described in the text. The horizontal lines indicate the α-helical content in a 1:1 TFE/buffer mixture of $^{196-214}$PC-TP (dotted line) and $^{183-214}$PC-TP (dashed line). Error bars represent ±one standard deviation for four experiments.

DISCUSSION

Structure−function analyses of human PC-TP require a facile system for expression, purification, and mutagenesis of recombinant protein. Because our previous attempts to express recombinant bovine PC-TP in *E. coli* were unsuccessful, we utilized a baculovirus/Sf9 expression system (*16*) to express and characterize recombinant human PC-TP. This approach yielded active protein, which could be readily purified. Although the baculovirus/Sf9 system expression system did permit expression of recombinant PC-TP, the relatively cumbersome methodology for producing recombinant PC-TP baculovirus and the modest protein yield (0.5 mg of purified protein/L of culture) led us to revisit the feasibility of protein expression in *E. coli*. In the absence of antibodies to bovine PC-TP, our previous unsuccessful attempts to detect PC transfer activity in *E. coli* cytosol for bovine PC-TP cloned into a pET3 overexpression vector (Novagen) led us to speculate that PC-TP could not be produced by *E. coli* (*16*). Under the current experimental conditions, however, we were able to detect low levels of activity in *E. coli* cytosolic proteins following expression of human PC-TP (Figure 2), and immunoreactive protein was detected on Western blot analysis with antibodies raised to recombinant human PC-TP produced using baculovirus. This suggested the possibility that an *E. coli* expression system could be optimized for expression of recombinant human PC-TP.

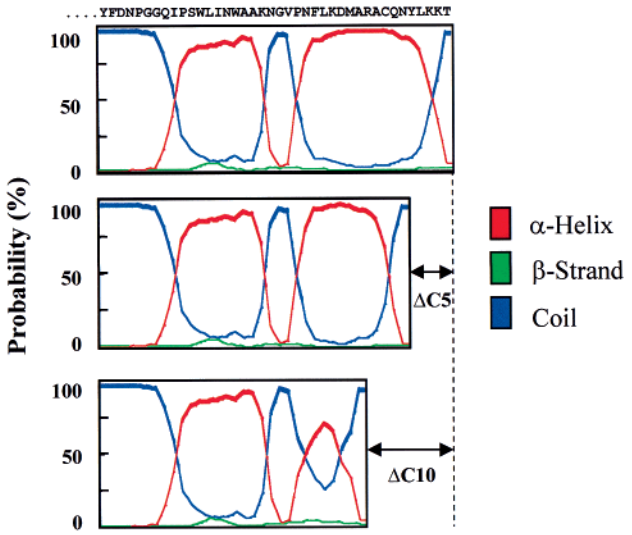

FIGURE 7: Predicted secondary structure (*26*) for the C-terminus of wild-type PC-TP (top) as well as truncation mutations ΔC5 (middle) and ΔC10 (bottom).

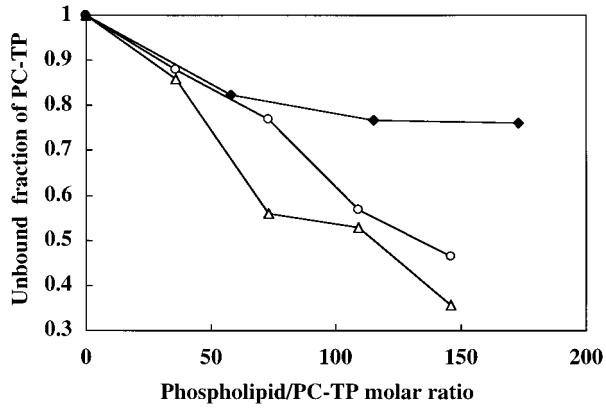

FIGURE 8: Binding of wild-type and truncated PC-TPs to SUV. Wild-type PC-TP (○), ΔN10 (△), and ΔC10 (◆) (5 μM) were incubated with increasing concentrations of SUV (80:20 PC:PS molar ratio). Unbound protein fractions were separated by ultrafiltration and quantified by slot−blot analysis. Each point represents the mean of two determinations.

Among the factors that may hinder heterologous expression of proteins in *E. coli* are differences between eukaryotic and prokaryotic codon usage (*32*). To explore whether this was true for PC-TP, we analyzed the ORF for human PC-TP by determining its codon adaptation index (CAI) as defined by Sharp and Li (*33*). The CAI predicts the likelihood that a heterologous gene will be expressed in a microorganism (e.g., *E. coli* or yeast) based on relative synonymous codon usage. Genes with CAI values of ≤0.30 are poorly expressed, whereas highly expressed genes have CAI values of ≥0.46. The CAI value of the native human PC-TP gene was 0.25, suggesting that unfavorable synonymous codon usage might indeed have been a limiting factor for expression of PC-TP in *E. coli*. By redesigning the ORF of PC-TP according to preferred codon usage for *E. coli* (*33*), we achieved a CAI value of 0.70 for the synthetic gene in Figure 1. Use of this gene resulted in a marked increase in the level of expression and yield of purified recombinant PC-TP and facilitated the production of mutated PC-TPs for structure−function analyses.

Activity of PC-TP is dependent upon transient interactions of the protein with membrane bilayers during transfer or exchange of PC molecules (*1*). Using phenyl isothiocyanate as a reagent to modify amino groups in the presence of membranes, van Loon et al. (*34*) identified K55 of bovine PC-TP as an amino acid residue that might participate in membrane binding. However, the authors could not distinguish this from the possibility that the residue was a component of the PC recognition site. Sterol carrier protein 2 and phosphatidylinositol transfer protein are the proteins in addition to PC-TP that promote intermembrane PC transfer in cytosol of mammalian cells (*1*). These lipid transfer proteins also interact with membranes, and recent studies have demonstrated that membrane binding may be attributable to α-helices situated close to the N- or C-terminus. Structural analysis of sterol carrier protein 2 by NMR has demonstrated the presence of two amphipathic α-helices near the N-terminus (*35*), and studies of peptides comprising these helices have provided convincing evidence for their role in membrane interactions (*22*, *36*). Similarly, an α-helical domain near the C-terminus (*37*) of phosphatidylinositol transfer protein appears to be required for membrane binding (*38*).

Data presented in this study suggest that the C-terminus of human PC-TP participates in membrane interactions. To identify potential amphipathic α-helices within the amino acid sequence of PC-TP, we applied a recently developed computer algorithm that utilizes neural networks to provide accurate predictions of secondary structure for a wide variety of proteins (*26*). By sequence alignment, van Helvoort et al. (*5*) demonstrated that the deduced amino acid sequences of the four cloned PC-TP orthologs (murine, rat, bovine, and human) are highly conserved (>77% identical, >84% similar). Consistent with this observation, the computer algorithm predicted similarly located α-helices for each species, as well as an additional α-helix near residue 30 of mouse, rat, and bovine PC-TPs. These findings are in general agreement with an earlier prediction by Akeroyd et al. (*10*) for the secondary structure of bovine PC-TP based on the methods of Chou and Fasman (*39*) and of Lim (*40*). However, this study did not predict the presence of the α-helix at residues 184−193, which was identified as α3 in the current study. This is an important distinction because an analysis of each predicted α-helix according to the method of Eisenberg (*29*) (Figure 4) suggested that the two α-helices situated near the C-terminus (i.e., α3 and α4) were the most likely to interact with membranes.

Experimental support for a C-terminal membrane interacting domain was gleaned from mutational analysis and from circular dichroism studies. Deletion of five residues (ΔC5) decreased PC-TP activity by ~50% (Figure 3B). As shown in Figure 7, this mutation reduced the length of α4 from 15 to 10 amino acids (residues 198−207). Because the ΔC5 deletion did not substantially alter the calculated mean hydrophobicity (−0.12) or hydrophobic moment (0.74), the foreshortened helix still plotted within region I of Figure 4. This observation could explain the partial retention of PC transfer activity by the ΔC5 mutant as compared with the ΔC10 deletion, which eliminated PC transfer activity of PC-TP (Figure 3B), abolished the predicted C-terminal α-helix (Figure 7), and markedly impaired binding to SUVs (Figure 8).

Measurements of circular dichroism for $^{196-214}$PC-TP and $^{183-214}$PC-TP in the absence and presence of TFE demonstrated the formation of α-helices (Figure 5) with helical contents that closely matched prediction values. Formation of α-helices was also promoted by addition of SUVs (Figure 6), indicating interactions between peptides and membrane bilayers. Because the amino acid sequences of $^{196-214}$PC-TP and $^{183-214}$PC-TP and the corresponding sequences of bovine PC-TP are nearly identical, as are their predicted secondary structures, inferences concerning the contributions of these peptides to protein function could be drawn from earlier functional studies of purified bovine PC-TP. Somerharju et al. (*41*) have shown that low concentrations of phosphatidic acid stimulate PC transfer activity by promoting interactions between bovine PC-TP and membranes. In contrast, higher concentrations of negatively charged phospholipids decrease activity by increasing the association constant of PC-TP with the membrane (*42*−*44*). This reduces the free fraction of PC-TP that is available in solution to transfer PCs between membranes (*41*). Accordingly, we found a tight inverse correlation ($R^2 = 0.97$) between the helical content of $^{196-214}$PC-TP (Figure 6C) and the activity of purified bovine PC-TP as measured by Wirtz et al. (*45*), each of which varied as a function of SUV PS content. This further supports the possibility that α4, the surface-seeking α-helix of PC-TP (Figure 4), mediates binding of PC-TP to membranes.

Using PCs into which photolabile fatty acids were incorporated at the sn-2 position, Wirtz and colleagues (*46*, *47*) identified binding to residues 171−177. On the basis of their earlier prediction of secondary structure (*10*), these investigators postulated that the lipid binding site of PC-TP includes an antiparallel β-sheet formed by hydrophobic β-strands at residues 171−177 and 182−190. Rather than forming a β-sheet, our data (Figures 5 and 6B) suggest that residues 184−193 form an α-helix, α3. Because the corresponding values for mean hydrophobicity and hydrophobic moment are close to those characteristic for membrane-spanning α-helices (Figure 4), this peptide might penetrate the membrane bilayer. When compared with $^{196-214}$PC-TP, the absence of variations in helical content of $^{183-214}$PC-TP as a function of SUV PS content (Figure 6C) suggests that the tendency for α3 to penetrate membranes dominates the behavior of the longer synthetic peptide, $^{183-214}$PC-TP.

In addition to the observation that membrane binding of the ΔN10 mutant was preserved (Figure 8) despite the loss of activity (Figure 3B), several additional lines of evidence argue against a critical role for the N-terminus in membrane bilayer association. (1) Sequence alignment of the four cloned PC-TP orthologs (murine, rat, bovine, and human) (*5*) has demonstrated that amino acids 2−6 are poorly conserved residues among otherwise very highly conserved sequences. (2) Deletion of nonconserved residues 2−6 (i.e., ΔN5 mutant) did not appreciably reduce PC transfer activity of recombinant human PC-TP (Figure 3B). (3) For each ortholog, a random coil is the predicted secondary structure of the first nine amino acids (data not shown). (4) Although the ΔN10 mutant displayed no PC transfer activity (Figure 3B), this truncation mutation did not significantly affect the predicted existence of α1 (data not shown). (5) Figure 4 shows that α1 is most characteristic of an α-helix within a globular protein. (6) Neither the presence of GST nor a His-tag at the N-terminus altered the activity of wild-type or mutated PC-TPs.

Taken together, studies of truncation mutants and synthetic peptides have provided evidence that the C-terminus of PC-TP may function as a membrane interaction domain involving an amphipathic α-helix. A closely situated hydrophobic α-helix might then penetrate the membrane bilayer, presumably to initiate binding of the fatty acyl chain(s) of a PC molecule. The lack of activity of the ΔN10 mutant indicates that membrane binding may be necessary but is not sufficient for PC transfer and that a more detailed understanding of PC-TP structure will be required to discern the contribution of the N-terminus to transfer activity. The facile method described in this study for achieving high-level expression of recombinant human PC-TP in *E. coli* should prove useful in studies designed to elucidate the structural basis for binding and intermembrane transfer of PCs.

ACKNOWLEDGMENT

We gratefully acknowledge expert advice and facilities provided by the Laboratory for Macromolecular Analysis at the Albert Einstein College of Medicine (Dr. Ruth Hogue Angeletti, director). We thank Dr. Friedhelm Schroeder for helpful discussions, as well as Drs. Ruth Stark and Wu Guohua for facilities and assistance with quasielastic light scatting measurements. The assistance of Steven Moyer and Marko Alsaygh is acknowledged.

REFERENCES

1. Wirtz, K. W. A. (1991) *Annu. Rev. Biochem. 60*, 73−99.
2. Cohen, D. E., Leonard, M. R., and Carey, M. C. (1994) *Biochemistry 33*, 9975−9980.
3. Smit, J. J. M., Schinkel, A. H., Oude Elferink, R. P. J., Groen, A. K., Wagenaar, E., van Deemter, L., Mol, C. A. A. M., Ottenhoff, R., van der Lugt, N. M. T., van Roon, M. A., van der Valk, M. A., Offerhaus, G. J. A., Berns, A. J. M., and Borst, P. (1993) *Cell 75*, 451−462.
4. Geijtenbeek, T. B. H., Smith, A. J., Borst, P., and Wirtz, K. W. A. (1996) *Biochem. J. 316*, 49−55.
5. van Helvoort, A., de Brouwer, A., Ottenhoff, R., Brouwers, J. F., Wijnholds, J., Beijnen, J. H., Rijneveld, A., van der Poll, T., van der Valk, M. A., Majoor, D., Voorhout, W., Wirtz, K. W., Elferink, R. P., and Borst, P. (1999) *Proc. Natl. Acad. Sci. U.S.A. 96*, 11501−11506.
6. Kamp, H. H., Wirtz, K. W. A., and van Deenen, L. L. M. (1973) *Biochim. Biophys. Acta 318*, 313−325.
7. Cohen, D. E., and Green, R. M. (1995) *Gene 163*, 327−328.
8. Kamp, H. H., Wirtz, K. W. A., Baer, P. R., Slotboom, A. J., Rosenthal, A. F., Paltauf, F., and van Deenen, L. L. M. (1977) *Biochemistry 16*, 1310−1316.
9. Akeroyd, R., Moonen, P., Westerman, J., Puyk, W. C., and Wirtz, K. W. A. (1981) *Eur. J. Biochem. 114*, 385−391.
10. Akeroyd, R., Lenstra, A., Westerman, J., Vriend, G., Wirtz, K. W. A., and van Deenen, L. L. M. (1982) *Eur. J. Biochem. 121*, 391−394.
11. Devaux, P. F., Moonen, P., Bienvenue, A., and Wirtz, K. W. (1977) *Proc. Natl. Acad. Sci. U.S.A. 74*, 1807−1810.
12. Berkhout, T. A., Visser, A. J. W. G., and Wirtz, K. W. A. (1984) *Biochemistry 23*, 1505−1513.
13. Kasurinen, J., van Paridon, P. A., Wirtz, K. W. A., and Somerharju, P. (1990) *Biochemistry 29*, 8548−8554.
14. Wu, M. K., Boylan, M. O., and Cohen, D. E. (1999) *Gene 235*, 111−120.
15. Cohen, D. E., Green, R. M., Wu, M. K., and Beier, D. R. (1999) *Biochim. Biophys. Acta 1447*, 265−270.
16. Feng, L., and Cohen, D. E. (1998) *J. Lipid Res. 39*, 1862−1869.
17. Cohen, D. E., and Carey, M. C. (1991) *J. Lipid Res. 32*, 1291−1302.

18. Boguski, M. S., Lowe, T. M., and Tolstoshev, C. M. (1993) *Nat. Genet. 4*, 332−333.
19. Westerman, J., Kamp, H. H., and Wirtz, K. W. A. (1983) *Methods Enzymol. 98*, 581−586.
20. Ikemura, T. (1985) *Mol. Biol. Evol. 2*, 13−34.
21. Dillon, P. J., and Rosen, C. A. (1990) *BioTechniques 9*, 298−300.
22. Huang, H., Ball, J. M., Billheimer, J. T., and Schroeder, F. (1999) *Biochemistry 38*, 13231−13243.
23. Cohen, D. E., Fisch, M. R., and Carey, M. C. (1990) *Hepatology 12*, 113S−122S.
24. Bradford, M. M. (1976) *Anal. Biochem. 72*, 248−254.
25. Laemmli, U. K. (1970) *Nature 227*, 680−685.
26. Chandonia, J. M., and Karplus, M. (1999) *Proteins 35*, 293−306.
27. Wada, K., Wada, Y., Doi, H., Ishibashi, F., Gojobori, T., and Ikemura, T. (1991) *Nucleic Acids Res. 19* (Suppl.), 1981−1986.
28. Coligan, J. E., Dunn, B. M., Ploegh, H. L., Speicher, D. W., and Wingfield, P. T. (1996) *Current Protocols in Protein Science*, John Wiley & Sons, New York.
29. Eisenberg, D. (1984) *Annu. Rev. Biochem. 53*, 595−623.
30. Eisenberg, D., Schwarz, E., Komaromy, M., and Wall, R. (1984) *J. Mol. Biol. 179*, 125−142.
31. Sonnichsen, F. D., Van Eyk, J. E., Hodges, R. S., and Sykes, B. D. (1992) *Biochemistry 31*, 8790−8798.
32. Makrides, S. C. (1996) *Microbiol. Rev. 60*, 512−538.
33. Sharp, P. M., and Li, W. H. (1987) *Nucleic Acids Res. 15*, 1281−1295.
34. van Loon, D., Westerman, J., Akeroyd, R., and Wirtz, K. W. (1986) *Eur. J. Biochem. 157*, 347−350.
35. Garcia, F. L., Szyperski, T., Dyer, J. H., Choinowski, T., Seedorf, U., Hauser, H., and Wuthrich, K. (2000) *J. Mol. Biol. 295*, 595−603.
36. Huang, H., Ball, J. M., Billheimer, J. T., and Schroeder, F. (1999) *Biochem. J. 344*, 593−603.
37. Voziyan, P. A., Tremblay, J. M., Yarbrough, L. R., and Helmkamp, G. M., Jr. (1996) *Biochemistry 35*, 12526−12531.
38. Tremblay, J. M., Voziyan, P. A., Helmkamp, G. M., Jr., and Yarbrough, L. R. (1998) *Biochim. Biophys. Acta 1389*, 91−100.
39. Chou, P. Y., and Fasman, G. D. (1978) *Adv. Enzymol. Relat. Areas Mol. Biol. 47*, 145−148.
40. Lim, V. I. (1974) *J. Mol. Biol. 88*, 873−894.
41. Somerharju, P., Brockerhoff, H., and Wirtz, K. W. A. (1981) *Biochim. Biophys. Acta 649*, 521−528.
42. Machida, K., and Ohnishi, S.-I. (1978) *Biochim. Biophys. Acta 507*, 156−164.
43. van den Besselaar, A. M. H. P., Helmkamp, G. M., and Wirtz, K. W. A. (1975) *Biochemistry 14*, 1852−1858.
44. Berkout, T. A., van den Bergh, C., Mos, H., de Kruijff, B., and Wirtz, K. W. A. (1984) *Biochemistry 23*, 6894−6900.
45. Wirtz, K. W. A., Geurts van Kessel, W. S. M., Kamp, H. H., and Demel, R. A. (1976) *J. Biochem. 61*, 515−523.
46. Westerman, J., Wirtz, K. W., Berkhout, T., van Deenen, L. L., Radhakrishnan, R., and Khorana, H. G. (1983) *Eur. J. Biochem. 132*, 441−449.
47. van Loon, D., Berkhout, T. A., Demel, R. A., and Wirtz, K. W. A. (1985) *Chem. Phys. Lipids 38*, 29−39.

BI001076A